Article

An Experimental Study of Mortars with Recycled Ceramic Aggregates. Deduction and Prediction of the Stress-Strain.

F. Guadalupe Cabrera-Covarrubias [1], J. Manuel Gómez-Soberón [2,*], J. Luis Almaral-Sánchez [3], S. Paola Arredondo-Rea [3], M. Consolación Gómez-Soberón [4], and Ramón Corral-Higuera [3]

1 Barcelona School of Civil Engineering, Polytechnic University of Catalonia, C. Jordi Girona 1-3, Building C2, 08034, Barcelona, Spain; guadalupe.cabrera04@gmail.com

2 Barcelona School of Building Construction, Polytechnic University of Catalonia, Av. Doctor Marañón 44-50, 08028, Barcelona, Spain; josemanuel.gomez@upc.edu

3 Faculty of Engineering Mochis, Autonomous University of Sinaloa, Fuente de Poseidón y Ángel Flores s/n, Col. Jiquilpan, Module B2, Los Mochis, Sinaloa, Mexico; jalmaral@uas.edu.mx; paola.arredondo@uas.edu.mx; ramon.corral@uas.edu.mx

4 School of Civil Engineering, Metropolitan Autonomous University, Av. San Pablo No. 180, Col. Reynosa Tamaulipas, 02200, Delegación Azcapotzalco, Distrito Federal, Mexico; cgomez@correo.azc.uam.mx

* Correspondence: josemanuel.gomez@upc.edu; Tel.: +34-934-016-242

Abstract: The difficult current environmental situation, caused by construction industry residues containing ceramic materials could be improved by using these materials as recycled aggregates in mortars, with their processing causing a reduction in their use in landfill, contributing to recycling and also minimizing the consumption of virgin materials. Although some research is currently being carried out into recycled mortars, little is known about their stress-strain (σ-ε); therefore this work will provide the experimental results obtained from recycled mortars with recycled ceramic aggregates (with contents of 0, 10, 20, 30, 50 and 100%), such as: the density, the compression strength, as well as the σ-ε curves representative of their behavior. The values obtained from the analysis process of the results are those of: σ (elastic ranges and failure maximum), ε (elastic ranges and failure maximum), and Resilience and Toughness; in order to finally obtain, through numerical analysis, the equations to predict their behavior (related to their recycled content). At the end of the investigation it is established that mortars with recycled ceramic aggregate contents of up to 20% could be assimilated just like mortars with the usual aggregates, and the prediction equations produced could be used in cases of similar applications.

Keywords: recycled ceramic mortars, stress-strain of mortars, elasticity module of mortars, recycled ceramic aggregates, toughness of recycled mortars, resilience of recycled mortars, formulation of recycled mortar behavior by numerical simulation.

1. Introduction

The recycling of waste products from the ceramic industry is an important objective, being as it is an obstacle to achieving a sustainable society [1]. This industry produces bricks, paving and roof tiles, of which 2% are taken to landfill due to deficiencies, cracks or fissures. This makes their controlled elimination difficult and as a result they end up being the origin of a serious environmental problem [2]–[4].

As a consequence of the search for solutions to their processing and recycling, recycled ceramic aggregates (CA) are being researched as total or partial substitutes for the usual aggregates (UA) (in mortars as well as in concrete); these new applications use fractions of both coarse and fine sizes

[5][6], and also as a partial substitution of cement itself (sporadically reaching the adequate properties [2][3][7]–[19]). In short, all of this research contributes to recycling, to a closed life cycle in building materials, reduces the environmental impact by preventing the waste products from reaching the landfill, and minimizes the consumption of natural resources [4], [18]–[20].

Recent research into mortars with different replacement percentages of UA by CA aggregates, have concentrated their results on explaining their behavior in their fresh and hardened state, thereby trying to establish their real chances of possible practical application.

Regarding their fresh state, Bektas *et al.* [21] reports that the consistency of the recycled ceramic mortars (RCM) is modified according to the content of the CA in the coarse fraction; two types of mortars with CA replacing UA (10 & 20%) were studied, concluding that consistency decreases with the increase in use of CA (from 11 to 24% less with regard to the control sample). This behavior was explained by the high water absorption capacity of the CA (also validated by [5]), although all the studied variables were considered acceptable according to the norms.

If only the fine fraction of the CA is used (0.063 - 0.150 mm), Silva *et al.* [22] reported (using 5 & 10% CA) the opposite, concluding on this occasion that the mixing water needed to achieve the determined consistency decreases as the fine CA are increased; it is the size and content of the CA used which dictates this property on this occasion (this is also verified by previous results [16]).

Ay & Ünal [2] conclude in their study that the use of the CA in its fraction of ceramic powder (CePo) (as a cement replacement, with contents of 25, 30, 35 & 40%), increases the consistency and, as a result, the mixing water can be reduced. On the contrary, Turanli *et al.* [12], who used two different CAs with contents of 20%, needed to increase the amount of water, from 103% to 106% with respect to the reference mortar; however, in both cases the tolerance is acceptable according to ASTM C618. In a similar manner, Pereira-de-Oliveira *et al.* [17] (using brick CePo and roof tile CePo with replacements of 10, 20, 25, 30 and 40%) obtained (for the 40% replacement) a decrease of 4% in the consistency of brick CA and of 3% for roof tile CA, attributing this to the theoretical increase in the specific surface area of the mortar (fineness of the CePo).

Therefore, if the use of CAs in the RCM leads to a loss in their consistency, it can be expected that their modification (water content available for forming hydration products) may affect their later behavior in their hardened state. So, with an adequate consistency a foreseeable improvement in resistance can be guaranteed (compacting, which produces a higher density); the common thread of the behavior being that good consistency leads to high density, which in turn guarantees good resistance (desirable elastic behavior). Referring to the density of the RCM, factors such as the size of the aggregates, the amount of replacement and its contribution as a cementing material have been studied. For the first factor (replacing the fractions of 0.063-0.150 mm), reductions in density (2 to 4%, for replacements of 5 and 10%) occurred [22]. For the second factor, Jiménez *et al.* [20] using replacements of 5, 10, 20, and 40%, and Kumavat & Sonawane [19], who used 5, 10, 15, 20, 25, 30, 35 and 40%, arrived at similar conclusions: contents of less than 10% CA do not imply significant variations (less than 1%), contents of up to 20% CA reduce their density (3%), and with 40% CA may reach 5%; diverging from the previous, Silva *et al.* [5] with replacements of 20, 50, and 100% reported more losses of density in all cases. Finally, the third factor indicates that the resulting density when using CA as a cementing material also follows the same principles; Kumavat & Sonawane [19] established density reductions of 3% when using a 40% mixture.

With regard to the properties of the RCM in their hardened state, the apparent density has experienced a similar trend to the density in fresh state; Silva *et al.* [5], Jiménez *et al.* [20] and Kumavat & Sonawane [19] report that their density decreases as the CA substitute the UA; similarly the density shows a slight decrease when the cement content is reduced (the cement/aggregate effect, c/a) and that of the CA increased [16]. This is explained by the lower density of the CA; therefore it is to be expected that in the σ-ε behavior of the RCM the replacement factor (density reduction) will also depend on this.

Porosity in the RCM has also been previously assessed, Corinaldesi [6] studied two cases (different distributions of particle sizes), in which 100% of the UA were substituted by CA. The distribution of pore sizes was studied as well as the total open porosity. The RCM with finer CA showed greater porosity (42% with respect to the control mortar and 5% more than the RCM with

coarse CA). Referring to the control mortar, analyzing the distribution of its pore sizes, it is shown that the micropore zone is reduced by 75 and 25% respectively, in the mesopore zone it was the same for the first case and rose by 14% for the second; and finally increased in the macrospore zone by 100 and 125% respectively, this last case generating the most notable difference in the CA (for both cases). In another study [11], with RCM containing 30% CA as cement replacement, it was shown that porosity was reduced with the passing of time (similar behavior to the control mortar). Additionally, if equally aged samples were compared, it could be seen that the RCM with cement replacing CA always showed greater open porosity; from which it can be deduced that the hydration process of CA is similar to that of cement, although less effective. In this particular case, the explanation is a question of the availability of hydration products and the abiliity to generate them. Likewise, Toledo Filho *et al.* [14] used CA in percentages of 10, 20, 30 and 40% to replace UA and defining two types of mortars (with water/cement (w/c) of w/c = 0.40 and 0.50); it was reported that using up to 20% CA a greater amount of porosity was produced (9 and 13% respectively), behavior which was not clarified in the research. On the other hand, if both variables used in the study are compared, it can be seen that the variable with a higher quantity of water (w/c= 0.50) generally shows 30% more porosity (free water inside the matrix).

Therefore, it should be emphasized that the structure or porous network of a mortar should, intuitively, be a direct factor by which the transfer of tensions must be established; this being, therefore, a property which influences their elastic behavior and causes limitations in their resistance (possible deformation and low resistance capacity), or on the contrary favors it (increase in matrix rigidity).

Some properties have been established regarding the mechanical behavior of the RCM, among which three principles for compressive strength (fm) have been established: replacement of UA by CA, of UA by CA and use of CePo for a part of the cement, and of CePo by cement.

In the study of the total replacement of UA by CA, Corinaldesi & Moriconi [6], Corinaldesi [24] and Higashiyama *et al.* [25] carried out studies on RCM, in which they used: CA of new red bricks (c/a = 1:3), crushed brick (c/a = 1:3) and ceramic waste of electrical insulators (c/a = 1:2) respectively. In the first two studies the results were similar, showing that at 28 days losses of 39% were established in the first case and of 40 and 73% in the second (all referring to a reference sample and the latter two with different crushing processes for the CA). The first case was explained by the lower specific weight and the high water absorption of the CA fractions used in comparison with the UA; and for the second case it was shown that the use of different particle size (PS) distributions (caused by using different crushing systems) meant that the RCM had finer particles –crushed in a ball mill–, achieving lower resistance with respect to RCM with coarser particles –crushed in a jaw mill–. Finally, increases of up to 14% were reported in the third study, although this 'anomaly' was not considered conclusive –possibly being generated by the high c/a ratio used–.

Silva *et al.* [5] studied replacements of 20, 50 and 100%, Jiménez *et al.* [20] of 5, 10, 20 and 40%, Kumavat & Sonawane [19] from 5 to 40% in increments of 5%, and finally Bektas *et al.* [21] with replacements of 5, 10 and 20%; with the exception of the last, all concluded that for percentages below 30% (in some cases even 50%) the fm is equivalent or even superior to the reference sample. This increase is due to the pozzolanic reaction that the fine fraction of the CA may show ('filling' action in the mortar matrix), other possible chemical reactions which may lead to new crystal products, and other physical effects (absorption, form and roughness).

Above this "limit" of CA content, a resistance loss of up to 14% should be expected; these may be the result of the dosage method used (by volume), which underestimates the high porosity of CA.

Finally, for Bektas *et al.* with resistance loss (3% at 28 days) and contents lower than 20%, it was concluded that at later ages (12 months) this effect could even be reversed (slowed maturation process).

Regarding the second principle of research, Higashiyama *et al.* [25] show that RCM in which 100% of the UA is replaced by CA (PS = 5 mm), as well as 10, 20 and 30% replacement of cement by brick CePo (PS = 0.075 mm), cause increases in resistance of 11 and 3% (10 and 20% of brick CePo); on the contrary, there is a reduction of 37% if the 30% mix is used. These results are explained by the

possible pozzolanic reaction of the CePo; however, not all the implications of this work have been clarified with precision.

Finally, for the third principle, up to 40% replacement of brick CePo for cement has been used, revealing that the compressive strength decreases as the percentage of CA substitution increases. The maximum losses in this study were of 16 to 31% [2][19][23]; on the other hand, another study that used 20% of CePo established reductions of 14 and 22% (two types of CePo were used) in respect of the reference sample [12]; on this occasion, with equal content to that of the first studies, similar losses were registered.

Contrary results have also been reported, showing increases of 3% (use of brick CePo with calcined clay, at 28 days, with w/c = 0.4) when 20% of the cement was replaced [14]. On this occasion, it seems that the RCM benefitted from the w/c effect, for in an identical test but using w/c = 0.5 and for whatever percentage of replacement, the results always showed resistance loss. In a final study results were obtained which differed from all the previous ones; for a replacement of 30% of CePo, reductions of up to 42% were reported [11].

Several hypotheses could be obtained from all the previous studies –although none conclusive– ; it seems that variables such as the cooking temperature of the clay CA (potential pozzolanic capacity), the speed of its reaction or maturity (hydration process) and the blocking effect in the cementing matrix of the RCM (high density and closure of the porous network) may be involved in this behavior, but given the divergence and variability of the results and variables that intervene, it is necessary to research still further. On the other hand, it may be said that whatever the mechanism –chemical, physical or mechanical– that alters the properties of the compressive strength of the RCM, this will have a direct repercussion on their deformation behavior, as this connection in their behavior has already been established in the general ambit of concretes and mortars [25]–[27], and should also arise in the RCM.

Flexural strength is another property of interest in the study of the σ-ε behavior in agglomerate materials, which in the case of the RCM is expected to show particular considerations. Favorable replacements of CA for UA with values of up to 50% have been reported, without affecting the flexural strength; Jiménez *et al.* [20] obtained perceptibly greater strengths than the reference, achieving the greatest strength (8%) with a 40% CA mix (28 days). Silva *et al.* [5] obtained similar results, with replacements of 0, 20, 50 and 100% achieving favorable results up to 50% of CA (with 20% it obtained the greatest increase, of 13%). In the case of 100% substitution, losses of 6% were reported, becoming 17 and 58% respectively in other studies [23][6]. The previously mentioned strength increases are explained (for 20 and 40% replacement) by the contribution of the pozzolanic effect of the CA, or by physical effects such as their increase in porosity and angularity (caused by the crushing process), which cause the 'sticking effect' of the cement paste in them; this contributes to the increase in strength. However, with the use of 100%, its behavior can be understood due to the fact that with high CA contents the beneficial pozzolanic effect does not predominate in the behavior of the cementing matrix; it is the low specific weight, high absorption and porosity which finally establish this as 'the weak link' of the group.

In the case of using CA to replace cement, Ay & Ünal [2] studied replacements of 25, 30, 35 and 40%; Corinaldesi *et al.* [28] and Moriconi *et al.* [11] studied only 30%. They all reported strength losses for all the replacement percentages; although in the last of the studies it was argued that other aspects such as the mortar-brick adhesive strength was good (linked to the distribution of the pore sizes of the brick, or to the rheological behavior of the mortar in its mutual adherence). It is clear that the replacement of CA by cement does not equal the latter's hydration capacity; however the application may be justified for uses with low contents (assumable losses of strength) for the value that its environmental benefits bring.

Regarding the static σ-ε relationship of the RCM, little has been explained with respect to their habitual characteristics such as the establishment of the elastic range (Youn'g modulus, or the modulus of Elasticity (E)) or the plastic range; similarly their respective elastic deformation ($\varepsilon_{elastic}$) established at 40% of the maximum load of failure (0.40 fm), and their maximum deformation of failure ($\varepsilon_{max.}$) reached by the material before the failure is present (fm). Despite the previous, these parameters are considered fundamental in evaluating the mechanical characteristics of the materials

[29], and necessary for the design of constructive elements in which they are integrated; therefore, an eventual proposal of standardized use with mechanical objectives requires their study, determining and explanation.

By general agreement, E has been nominated as the ratio between for the increase of strength and the corresponding change to the unitary deformation of a material [30]; if the level of strength passes the elastic limit, then the material enters into the plastic range, characterized by displaying non-proportional increases in its deformation as a response to the increases in stress to which it is subjected. When the applied charge produces the failure in the material, the deformation at this instant is specified as the $\varepsilon_{max.}$ of the failure (see **Figure 1**).

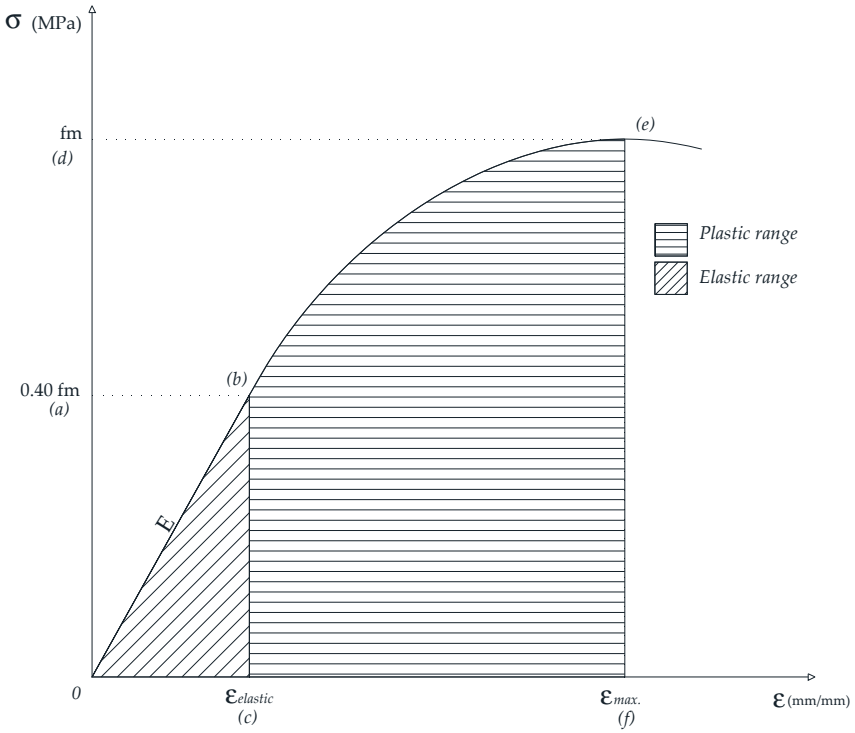

Figure 1. σ-ε curve diagram.

Static tests are the habitually used procedures for determining the σ-ε relationship of the materials, this being a mechanical characteristic, which leads to defining them in several aspects (elasticity, plasticity, malleability and hardness). The diagram σ-ε is unique for each particular material; but these can be classified in two different types of materials: ductile materials (showing large ε) and fragile materials (showing small ε) [31]. From the diagram σ-ε it is possible to determine the E ('desirable' behavior of construction materials), which describes its relative rigidity. This property can be obtained through a laboratory test in which the slope of the elastic region of the diagram σ-ε [32] is determined; numerically this is obtained from the coefficient of the strength regarding the unitary elongation [33] as can be seen in equation (1):

$$E = \sigma/\varepsilon = \frac{F/A_0}{\Delta L/L_0} = FL_0/A_0\Delta L \quad (1)$$

Where, *E* (in MPa) is Young's Modulus; *F* (in N) is the applied axial force; *Ao* (in mm²) is the area of the original transversal section; *ΔL* (in mm) is the variation of the longitudinal dimension of the object and *Lo* (in mm) is the original height.

Regarding previous results of E for the RCM, some particular variables of their study have been reported. The first has been the partial use of CA as a substitution for cement in percentages of maximum values of up to 40%. Moriconi *et al.* [11], applying static compression tests and with the diagram curve σ-ε, showed losses at all ages of the study, the maximum being at 28 days (46% with respect to the reference); with similar results Toledo Filho *et al.* [14] reported that E decreases

inversely to the increase in the percentage of replacement of CA; with substitutions of 0, 10, 20, 30 and 40%, decreases of 3, 5, 7 and 9% over the control mortar (at 28 days, w/c = 0.5). However, with w/c = 0.40 similar behavior to the previous was obtained, with the exceptions being mortars with 10 and 20% CA, which showed an increase in E of 1 and 2% respectively, both with reference to the control mortar. Therefore, it seems that the replacement factor is adverse and the w/c relationship is less decisive (within the studied limits).

The second variable studied was the use of RCM with CA replacing different percentages of UA, in which losses have also been reported; for example Silva *et al.* [16] reported decreases of E when 10% of CA was replaced (the variables of c/a studied were = 1:6 and 1:4), indicating as the most important result that the effect of c/a could be similar (18 and 17% of losses respectively) at prolonged ages (2 to 5 months); and the behavior was held responsible for the formation of fissures, showing that a lesser E permitted lower internal tensions for identical deformations. In parallel works [5], an experimental campaign was defined with c/a = 1:4 but now arriving at replacement values of CA by UA of 50%; on this occasion the losses indicate values of up to 40% with respect to the reference sample (at 2 as well as at 5 months), concluding that the application of monolayer mortar in the walls may be appropriate –if these losses are accepted–.

As the third variable studied, total replacements of CA were made, both for UA and for the cement; Higashiyama *et al.* [24] used two different PS of CA in their study, using 100% CA as an aggregate and studying replacements of 10, 20 and 30% for cement. On this occasion, for the RCM with 10 and 20% cement replacement, increases of 2 and 5% respectively were obtained with regard to the reference samples, this behavior being explained by the good mechanical qualities of the CA; however, in the case of the variable that used 30%, losses of 6% were reported –the reason has not been fully clarified–.

Based on the previous, the objective of this research is to determine more precisely all the σ-ε relationships that the RCM could contain due to the effect of the replacement of their UA by different percentages of CA; as a result the experimental methodologies have been established for: aggregate substitution procedures, mortar mixing protocol, static mechanical and deformation spotting tests and, finally, the numeric analysis of data which allows the real values of their σ-ε behavior to be established, such as the fm, 0.40 fm, $\varepsilon_{elastic}$, $\varepsilon_{max.}$, E, toughness (T) and resiliency (U_r); as well as their particular prediction equations.

2. Materials and methods

2.1. Materials and mortar dosage

CA was available as an aggregate for use in the study of the RCM, obtained from a treatment plant for aggregates from waste and demolition, which in turn came from a local company that supplied ceramic roof tiles for the construction industry; the material was eliminated from the production process for not meeting the requirements (defects in size or faults in their geometry). The material used had a PS of between 0 - 5 mm. As UA, a silica sand, from a local supplier of natural aggregates for construction, was used (PS of 0 - 4 mm). The physical properties of the aggregates used are shown in **Table 1**; the bulk density values in oven-dry condition (M_{OD}), the bulk density in saturated-surface-dry condition (M_{SSD}) and the void content correspond to the materials used; on the other hand, the Density values in oven-dry condition (D_{OD}), Density in saturated-surface-dry condition (D_{SSD}), absorption (more significant in this case), fineness modulus and particles of less than < 75μ correspond to the aggregates finally used in the research –the granulometric profiles being adjusted to the limits ASTM C144 [34]–, which consists in dividing the original profiles into two fractions (Sieve No. 30, 0.59 mm) in the search for the maximum bulk density. The CA was made up of 60% of the material retained in the sieve and 40% of the that passes through the sieve; in the case of the UA the optimal adjustment was made using 50% of each material, the retained and the sieved.

Of the tests carried out, in agreement with others [5][19][20], the density of the CA was inferior to that of the UA, being 24% less on average (in general). The opposite was the case for absorption,

in which the CA were up to 12 times bigger than the UA –similar to others reported previously [5][6][20]–.

Table 1. Physical properties of aggregates.

Property [1]	CA	UA
Without adjusted granulometric profiles		
M_{OD} (Kg/m^3)	1182.0	1735.1
M_{SSD} (Kg/m^3)	1399.1	1860.8
Void content (%)	35.3	32.9
With adjusted granulometric profiles		
D_{OD} (Kg/m^3)	1820.9	2581.6
D_{SSD} (Kg/m^3)	2155.4	2623.6
Water absorption coefficient (%)	18.4	1.6
Fineness modulus materials	2.8	2.4
Particles < 75-μm (sieve No. 200) (%)	8.2	2.9

[1] According to ASTM (C128 [35], C136 [36] y C117 [37]).

Portland cement CEM I 42.5 N/SR (UNE EN 197-1:2011 [38]) was used as a binder, being commonly used and having the usual properties and components; and finally potable tap water was also used in making the mixtures.

2.2. Experimental campaign/specimens

Test specimens of 4 cm x 4 cm x 16 cm were made with different material contents, the percentages of CA used to substitute the UA were identified as: UM (usual mortar), which refers to the mortar in which only UA was included (0% CA); and RCMXX%, which refers to the RCM in which a part of the UA are replaced (XX%, in weight) by CA. The total of the study variables to be compared with the UM were designated thus: RCM10, RCM20, RCM30, RCM50 and RCM100 (10%, 20%, 30%, 50% and 100%).

Table 2 presents the characteristics and proportions for obtaining a dm^3 of each of the study mixes used in the research; all the mixtures were designed with a c/a ratio of 1:4 and of w/c = 0.5 initially. The dosage process was carried out in accordance with the criteria generally accepted in previous studies: the recycled aggregates required previous saturation to prevent the movement of water necessary for hydration [39][40]. The mixing sequence and the duration of the process included the following phases: introduction of the UA and/or CA and the total water content of the mixture into the mixer (brand Matest, Mod. E93.), leaving the materials to soak for a minute before introducing the cement; then they are mixed for one minute at medium speed, followed by 30 seconds at high speed, another 90 at rest and finally mixing for one more minute at high speed. Before molding the test specimens, the compliance of the properties in fresh state (ASTM C230 [41], C231 [42]) is verified.

Table 2. Characteristic and proportions of the mixtures of studio.

Materials (g)		Classification and proportions of the mixtures					
		UM	**RCM10**	**RCM20**	**RCM30**	**RCM50**	**RCM100**
Water		334	390	355	373	397	476
Cement		400	433	381	372	348	323
UA [1]	< Sieve No. 30	800	780	610	521	348	0
	> Sieve No. 30	800	780	610	521	348	0

Preprints (www.preprints.org) | NOT PEER-REVIEWED | Posted: 28 November 2016 doi:10.20944/preprints201611.0143.v1

Peer-reviewed version available at Materials 2016, 9, 1029; doi:10.3390/ma9121029

CA [1]	< Sieve No. 30	0	69	122	179	278	517
	> Sieve No. 30	0	104	183	268	417	775

[1] Dry condition.

Once the mixture is completed the resulting product is introduced into the molds, leaving them for 24 hours in a humidity chamber (Relative Humidity close to 95%); subsequently they are removed from the molds and submerged in water to keep them saturated until their test age.

2.2. Details of tests and procedures

For determining the density of the RCM, the prescription of UNE EN 1015-10 [43] and UNE EN 1936 [44] were used, also using for this study the remaining half of a specimen previously subjected to a flexural test at an age of 60 days (considering that this property has reached stability of maturity at this stage).

The fm and the σ-ε curve were obtained at the age of 90 days (sufficient maturity for the aims of the study) in test specimens that had previously been removed from their curing process in water. Three specimens of each variable were used for the compression test, using half of the specimen remaining from the previous flexural test (3 specimens per variable) in accordance with ASTM C349 [45].

The σ-ε curve necessary for determining E was obtained during the compression strength test; for which it was decided to use a linear displacement sensor (LSC Transductor, MPE brand), connected to the universal press (5000 KG Stepless Compression Test Machine, by Wykeham Farrance Ltd., England) with the aim of establishing the deformation produced by the effect of the load on the specimen. An external load cell (5t ± 2mV/V, HBM brand) was used to establish the amount of charge applied to the specimen; both instruments (transductor and charge cell) were connected to a data acquisition unit (model SCXI-1000, brand NATIONAL INSTRUMENTS), which sends the acquired data to a computer; this is later processed and finally the graph of the σ-ε curve is generated. **Figure 2** shows the experimental setup used, and in **Figure 3** there is an example of the resulting graph, the vertical axis (Y) indicating the values of the charge in kg, and the horizontal axis (X) showing the deformation in cm.

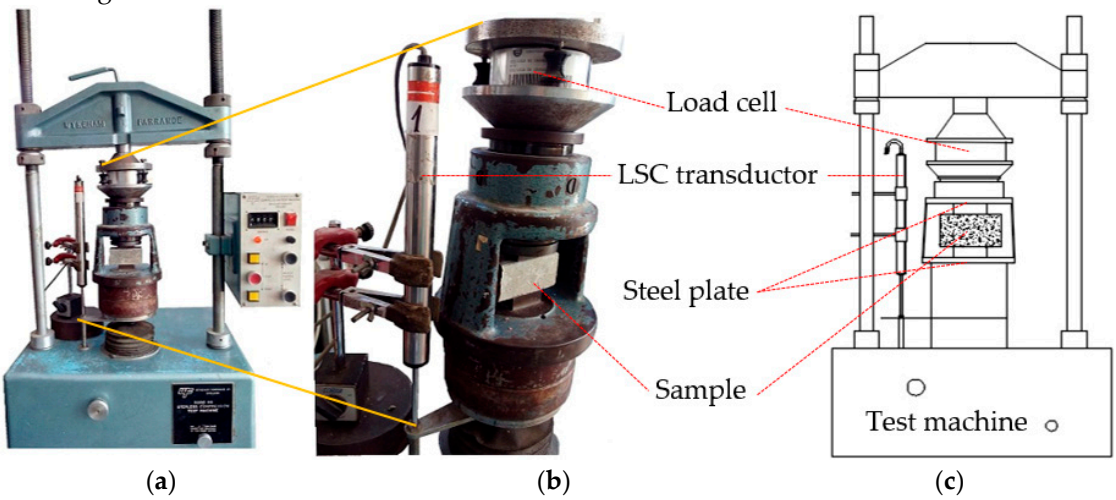

Figure 2. (**a**) General configuration of the experimental arrangement; (**b**) Detail of LSC; (**c**) Idealized scheme from set.

Preprints (www.preprints.org) | NOT PEER-REVIEWED | Posted: 28 November 2016 doi:10.20944/preprints201611.0143.v1

Peer-reviewed version available at Materials 2016, 9, 1029; doi:10.3390/ma9121029

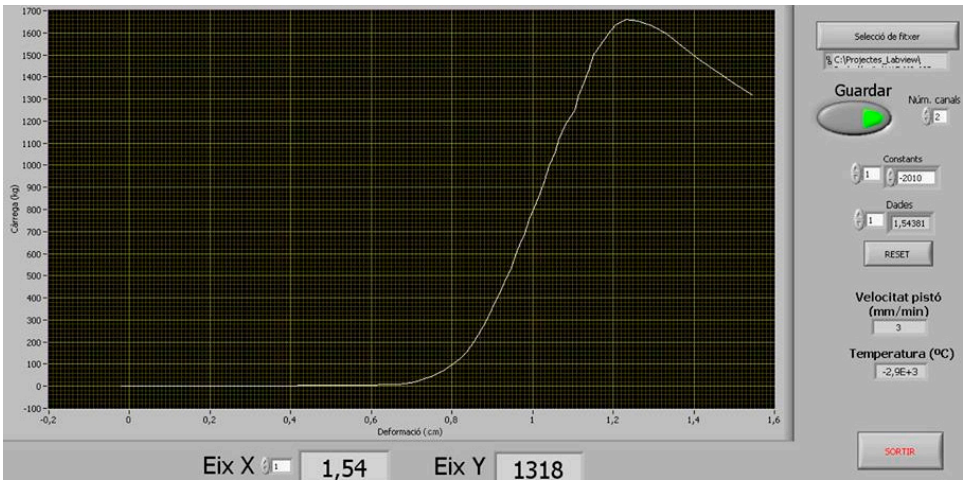

Figure 3. Curve σ-ε resulting from a test.

Once the data had been extracted from the computer, it was processed on a spreadsheet to obtain the σ-ε curves in accordance with **Figure 1**. As a working principle of the data capture system itself, a manual adjustment was necessary, which involved locating the starting point of the test. This was established in the following manner: the first pair of values σ and ε in which an ε > 0 (σ_2 with $\varepsilon_2 > 0$) was detected was considered to be the second pair of values of the test. Which therefore makes the previous values (σ_1 and ε_1) become $\sigma_1 = 0$ and $\varepsilon_1 = 0$. The rest of the pairs of σ and ε were then recalculated, in accordance with this principle of correction. The previous adjustment eliminates the initial semi-straight section of the curves, which had originated in the adjustments made at the start of the charge phase (adjustment of the charge plates, parallelism of the specimen faces, acquisition of LSC, etc.); and on the other hand it allows all the curves to be put at the same test starting point, thus making their comparison easier.

To continue with the information analysis, the value of fm was located, which was determined as the value of maximum tension reached prior to the tension decrease (specimen failure). Then, the value of 0.40 fm was determined, and was established as the limit between the elastic and the plastic behavior of the material. In both cases the projection that arose between these values on the vertical axis (fm and 0.40 fm) and the intersection with the σ-ε curve allowed the values of $\varepsilon_{max.}$ and $\varepsilon_{elastic}$ respectively to be established on the horizontal axis.

For the simplified determination of E the following procedure was established: obtain the slope of the theoretical straight line, created in the section limited by the intersection of the curve with 0.40 fm (point b of **Figure 1**) and the origin of the diagram (point 0 of **Figure 1**) [32]. Bearing in mind that the material deforms in the elastic range (without σ, its ε is recovered), the equation used to determine the slope was of linear type, with a constant slope. For its regression, all the pairs of values σ-ε contained within the previously established range were used. The equation (2) used is shown below:

$$y = ax + b \quad (2)$$

Where y is the dependent variable (σ, in MPa); a is the slope of the curve (E, in MPa), x is the independent variable (ε, in mm/mm) and b is the point where the slope cuts the "Y" axis (in MPa).

The area below the σ-ε curve has been defined as Ur [46], assigning to this area the concept of the energy which the test specimen of mortar is able to absorb or transform (in deformation), with a validity limit of up to an σ of 0.40 fm. For a numerical quantification, the area below the curves, limited by the points "0", "b" and "c" of **Figure 1**, was estimated.

Regarding T, this has been associated as the total energy absorbed or transformed in deformation by the test specimen of mortar of the entire curve σ-ε [32][47]; however, given the difficulties and implications of a correct capture of the section of the σ-ε curve after fm, only the area below the σ-ε curve, bounded by the points "0", "b", "e", "f" and "c" in **Figure 1,** have been considered. In both cases the area below the curves is obtained by use of the trapeze method, according to equation (3),

Peer-reviewed version available at Materials 2016, 9, 1029; doi:10.3390/ma9121029

for each pair of values of increase of σ and its respective ε, in order to get their sum and thereby obtain the total sought area below the curve.

$$\int_0^i f(x)dx = (\varepsilon_2 - \varepsilon_1)\left[\frac{\sigma_1 + \sigma_2}{2}\right] \quad (3)$$

Where ε_1 (mm/mm) is the lesser deformation of the pair of study values; ε_2 (mm/mm) is the greater deformation of the pair of study values; σ_1 (MPa) is the lesser stress of the pair of study values; σ_2 (MPa) is the greater stress of the pair of study values and *f(x)* (MPa) is the area below the σ-ε curve. Similarly, the secant modulus of elasticity (Eo) was determined from the origin of the coordinates to the corresponding point of maximum stress of its theoretical straight line. This was established by obtaining the slope of the theoretical straight line which is created in the section limited by the intersection of the curve with fm (point d) and the origin of the diagram (point 0) of **Figure 1**.

3. Results

There now follow the results obtained regarding density in hardened state, the compression strength, at E, U_r, and T, as well as the values of $\varepsilon_{max.}$ and $\varepsilon_{elastic}$ obtained from the experimental campaign described; a numerical - analytical process was then carried out with these results to determine the equations for predicting the behavior of the RCM for each of the studied properties, and finally the equations which define the theoretical behavior of the σ-ε curves have been established.

3.1. Density in hardened state

Table 3 shows the results of the density (ρ) obtained for the RCM studied; it can be noted how the RCM are always less heavy than the UM and, equally, their density is inversely correlative to the CA content. This is due to the density of the aggregates used (see **Table 1**).

Table 3. Density in hardened state of the RCM.

Study variables	ρ (g/cm³)
UM	1.950
RCM10	1.948
RCM20	1.894
RCM30	1.864
RCM50	1.798
RCM100	1.529

3.2. Compression strength

In **Figure 4** the values obtained from fm are presented for the different RCM studied, in which three zones of behavior can be observed: First (low content); similar values to those of UM are obtained for RCM10 and RCM20 (in this study, increases of 1.5% and 0.3% respectively), similar to that established in other studies which show increases of 1% in RCM with 20% of CA at 90 days [20] and losses below 3% with 10 and 20% of CA at 56 days [21]. Second (intermediate content); for samples RCM30 and RCM50 less resistance was found than in the case of the UM (6% and 14%), contrary to previous studies (50% CA use shows greater fm than the reference) [5][19][20]. Finally, for the third zone (maximum content), RCM100 has a marked loss with respect to the UM (loss of 35%), coinciding with other research [6][48] (39 and 40% less than the reference at 28 days with c/a = 1:3 and 1:2).

Preprints (www.preprints.org) | NOT PEER-REVIEWED | Posted: 28 November 2016 doi:10.20944/preprints201611.0143.v1

Peer-reviewed version available at Materials 2016, 9, 1029; doi:10.3390/ma9121029

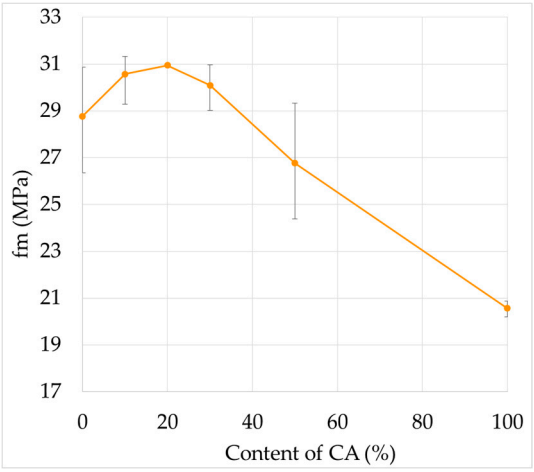

Figure 4. Compressive strength of the RCM at 90 days of age.

The explanatory hypotheses of the compressive behavior for the different CA contents are: For low CA contents there is a possibility that the strength increases are due to a pozzolanic reaction in the fine fraction of the CA, causing a 'filling' effect in the matrix and a reduction of the porosity (which improves strength). The validation of this hypothesis was corroborated by observing the matrix with a JEOL JSM-6510 scanning electron microscope (SEM). In the following

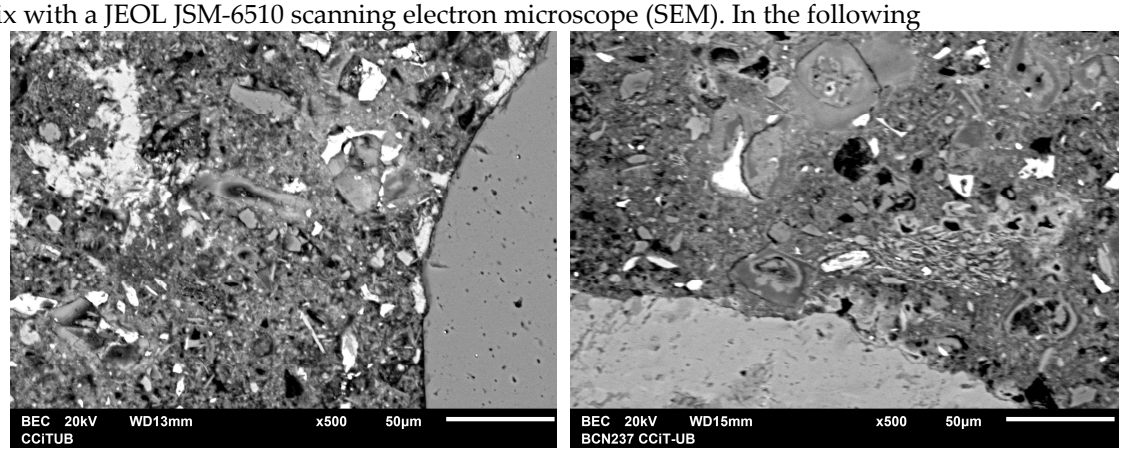

(**a**) (**b**)

Figure 5 the UA, CA, grout (G) and the interfacial transition zone (ITZ) can be seen; both in image a) UM and image b) RCM10. In image a) a wide ITZ can be seen around the UA, as well as a smoother UA profile (less adherence); while image b) shows a denser and more uniform (lower porosity) matrix, a thinner ITZ and a rougher CA.

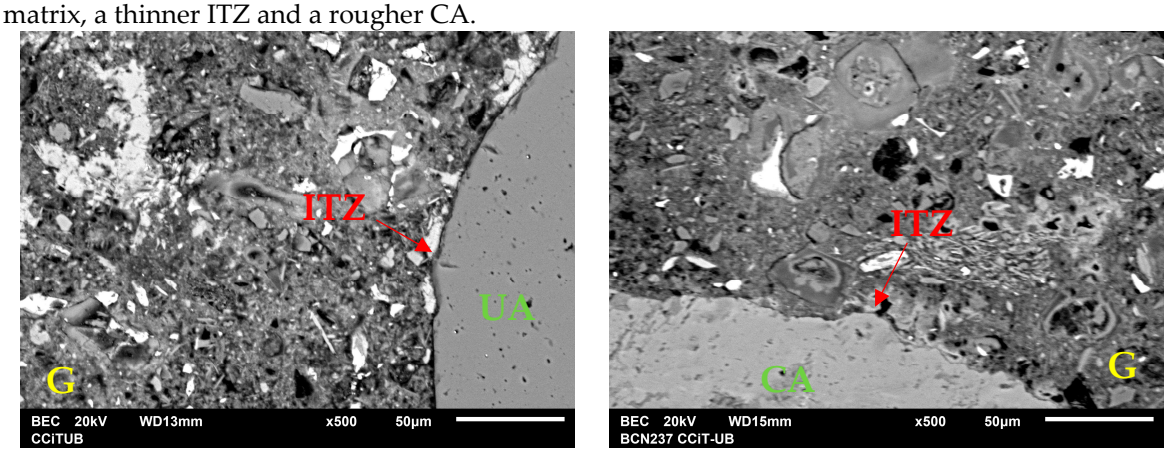

(**a**) (**b**)

Figure 5. (**a**) UM (0% of CA); (**b**) RCM10 (10% of CA).

Preprints (www.preprints.org) | NOT PEER-REVIEWED | Posted: 28 November 2016 doi:10.20944/preprints201611.0143.v1

Peer-reviewed version available at Materials 2016, 9, 1029; doi:10.3390/ma9121029

Additionally, another possible reason why the RCM show divergences in their strength is the method of proportioning used in their dosage (weight or volume); for example, when substituting materials according to weight a greater amount of inferior quality mortar is produced [20], due to the lower density of the recycled aggregate, which causes a lower strength. Regarding the RCM with strength losses, it is suggested that the increase in the CA content causes the pozzolanic reaction of the fine fraction to be lost (or annulled), leading to the unfavorable effects of lower density and high absorption of CA becoming dominant in the resistance behavior of the matrix (weaker and more porous). In **Figure 6** the samples a) RCM50 and b) RCM100 are shown; in both cases the ITZ is wider and G is disperse and non-homogenous; in particular, in b) a zone of high porosity can be seen around the CA, as well as the presence of microfissures (marked in the circumferences). **Figure 7** shows the location of the most usual components in mortar chemistry for the two samples referred to; the images were obtained through mapping and microanalysis by x-ray diffraction (XRD) connected to the SEM used. The preferred location refers directly to the origin of the CA, and the degree and chemical composition of the hydration attained by G and its porosity; they are distinguished by the juxtaposition in the images of the increase of the ITZ [in (a) and (b) for the compounds Al and Si], as well as an important amount of microfissures (bad adherence) of the RCM with high contents (see **Figure 6**b).

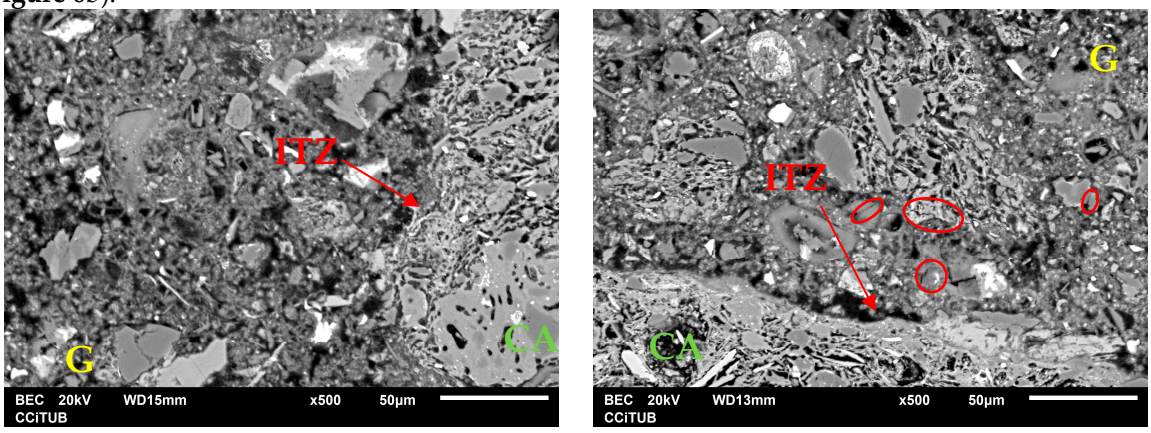

(**a**) (**b**)

Figure 6. SEM of: (**a**) RCM50 (50% of CA); (**b**) RCM100 (100% of CA)

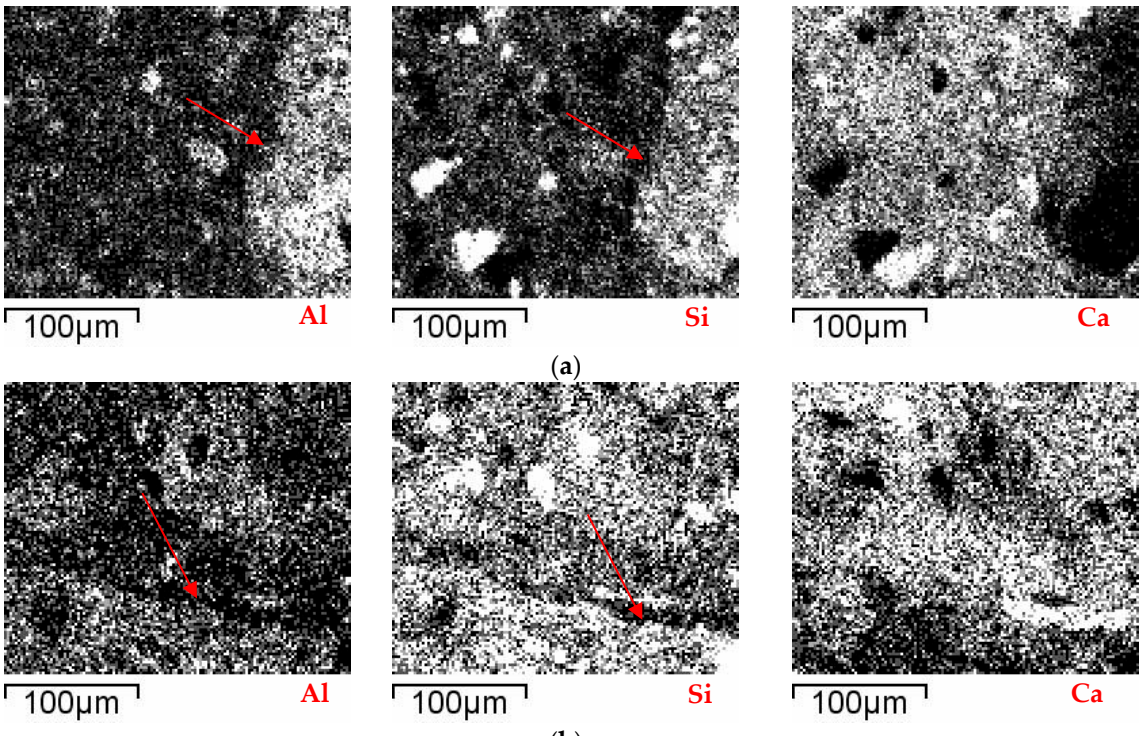

(**a**)

(**b**)

Peer-reviewed version available at Materials 2016, 9, 1029; doi:10.3390/ma9121029

Figure 7. Microanalysis of components by mapping in SEM of the majority compounds: (**a**) RCM50; (**b**) RCM100.

3.3. Calculation of E

Figure 8 shows the curves corresponding to the RCM with the different percentages of the studied CA up to a stress level equal to $\sigma_{max.}$ The E is determined from these curves (see test details).

In general it can be seen that the RCM10 and RCM20 show similar values to UM (similar behavior to fm); and with regard to the rest of the mixtures (CA content ≥ 30%), the E shows inversely proportional losses. Specifically, for the RCM10 there is an increase of 1%, while the RCM20 has the same value of E (when compared to the reference); for RCM with 30, 50 and 100%, the values of E suffered decreases of 8, 17 and 46% respectively.

The above mentioned trends are coherent with previous works (the case of using CA to replace cement) with different levels of loss of E (the maximum was 41% at 70 days) [11]; similarly, substitutions of 0, 10, 20, 30 and 40% of CA by UA with w/c mixtures of 0.4 and 0.5 show decreases of 3, 5, 7 and 9% at 28 days with w/c = 0.5; while for mortars with 10 and 20% of CA and w/c = 0.4 increases of 1 and 2% respectively were obtained [14] –similar to this study–. On the contrary, Higashiyama et al. [24] obtained values of E higher than the reference (2 and 5%) in mortars with 100% of CA and with 10 and 20% of CA as a cement replacement.

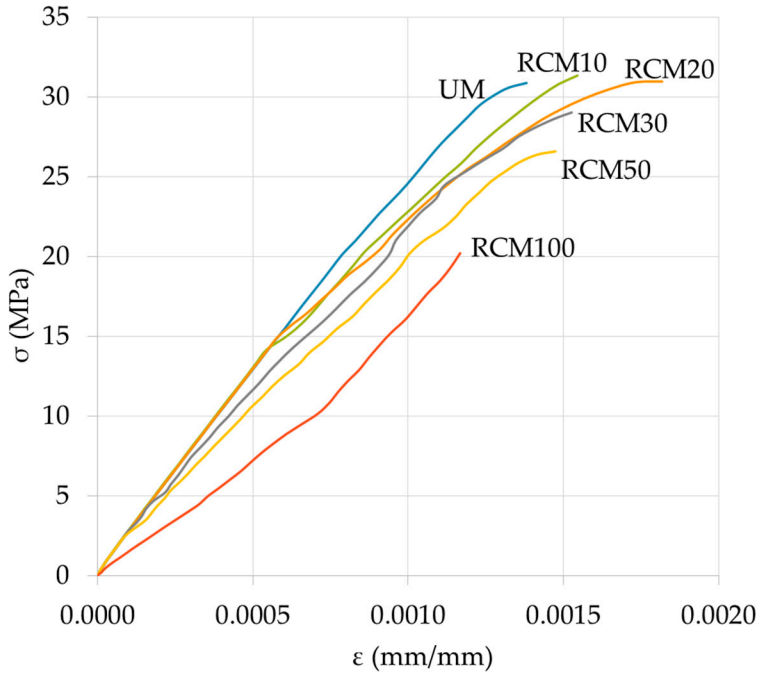

Figure 8. σ-ε curves of the RCM.

Compared with studies where percentages of the UA were replaced by CA (similar to this one) the results were contradictory; RCM with 10% of CA (c/a = 1:6 and 1:4; at ages of 2 to 5 months) showed losses of 18 and 17% respectively (similar values for the effect of c/a). The explanation for this was attributed to the forming of cracks, given that a lower value of E permits lower internal tensions for identical deformations [16]. Similarly, in another work by the same author, with replacement of 50% of CA by UA (c/a = 1:4 at ages of 2 and 5 months), the resulting losses were of 40% regarding the reference samples [5].

To sum up, it can be said that in this study the behavior of E is similar, in terms of its origin, its implications and its justification (the effect of the CA on the RCM), to the previously mentioned case of the property of fm (correlated and coherent properties, as occurs in the UM). However, it should be pointed out that in the previous works in which the E of the RCM was studied [5][16][22], this was determined by means of resonance vibration frequency according to the French norm NF B10-511F [49], which consisted in causing the specimen to vibrate until the resonance frequency was obtained,

with which it was then possible to determine the dynamic elasticity modulus through established equation; as a result, the scarcity of studies that obtain the E of RCM by means of the σ-ε curve is patent. As this provides knowledge in this field of study, until further data is obtained, a cautious comparison of the various studies is required.

From the curves in **Figure 8** the previously mentioned procedures were carried out in order to establish the behavior properties of σ-ε of the RCM (see **Table 4**). It can be appreciated that for T the values obtained have two clearly defined zones, limited by RCM20: before it, increases (the pozzolanic reaction effect of the CA) of up to 46% are seen; after it (high CA contents) the losses are of up to 42% (RCM100), in both cases regarding UM. Concerning U_r, the observed behavior is similar to that of T, with the difference that after RCM20 the losses are not proportional (linear decrease of T); meanwhile, in the case of U_r they undergo acceleration with the increase of CA. Therefore it can be expected that in the elastic range of the RCM the effect of the increase of CA will make it more likely for them to have a normal behavior or similar to a UM. Regarding $\varepsilon_{elastic}$, the values obtained from the different RCM may all be considered as constants (0.0005 mm/mm), thereby establishing this as the reference value for the use, design and calculation of mortar applications. For the RCM, regarding the $\varepsilon_{max.}$, the increases obtained with respect to $\varepsilon_{elastic}$ are on average 3.08 times bigger, with the greatest increase being in RCM20 (limit of the zone with pozzolanic reaction, with 3.60 times more). This means that the RCM would have a plastic deformation capacity of between 2.93 and 1.87 times more than, for example, the usual concrete; and comparing the average of all RCM with respect to the UM, the former will show 0.56 times less deformation. Therefore, it can be said that the RCM have a tendency to show more fragile failures than the UM. Finally, as regards the Eo, there is an evident loss of rigidity for all the CA contents, which is correlational with the increase of the CA content.

Table 4. Properties of σ-ε of the RCM.

Study variables	fm (MPa)	0.40 fm (MPa)	E (MPa)	T (MPa)	U_r (MPa)	$\varepsilon_{elastic}$ (mm/mm)	$\varepsilon_{max.}$ (mm/mm)	Eo (MPa)
UM	30.87	11.59	26252	0.024	0.003	0.0004	0.0014	23619
RCM10	31.33	11.89	26515	0.029	0.003	0.0005	0.0016	21710
RCM20	30.95	12.03	26251	0.035	0.003	0.0005	0.0018	20249
RCM30	29.02	11.58	24065	0.025	0.003	0.0005	0.0016	21107
RCM50	26.58	9.85	21731	0.022	0.003	0.0005	0.0015	18940
RCM100	20.20	7.66	14194	0.010	0.002	0.0005	0.0012	15891

Figure 9 shows the graphs corresponding to the results of σ-ε obtained from the RCM and the equations which best adjust the trends (coefficient of determination) referring to the replacement factor (RF, where RF = content of CA/100); the use of these correlations was decided upon in order to show the significance of the RF with respect to the properties of the RCM. As can be seen, the graphs corresponding to (a), (b), (c) and the variable $\varepsilon_{max.}$ in (d) generally tend to reduce their values as the RF increases, their best fitting curves being represented by second degree polynomial equations. Specifically, if the equations are aimed at the particular behavior of the properties studied, they could even establish two markedly different zones; for low RF (≤ 0.20) the RCM properties show values similar to —and even greater than– those of the UM, while for RF ≥ 0.20 the trend could be represented by a decreasing linear equation. Finally, in the case of $\varepsilon_{elastic}$ (d), in contrast to all the others the RF effect generates a generally increasing equation.

Preprints (www.preprints.org) | NOT PEER-REVIEWED | Posted: 28 November 2016 doi:10.20944/preprints201611.0143.v1

Peer-reviewed version available at Materials 2016, 9, 1029; doi:10.3390/ma9121029

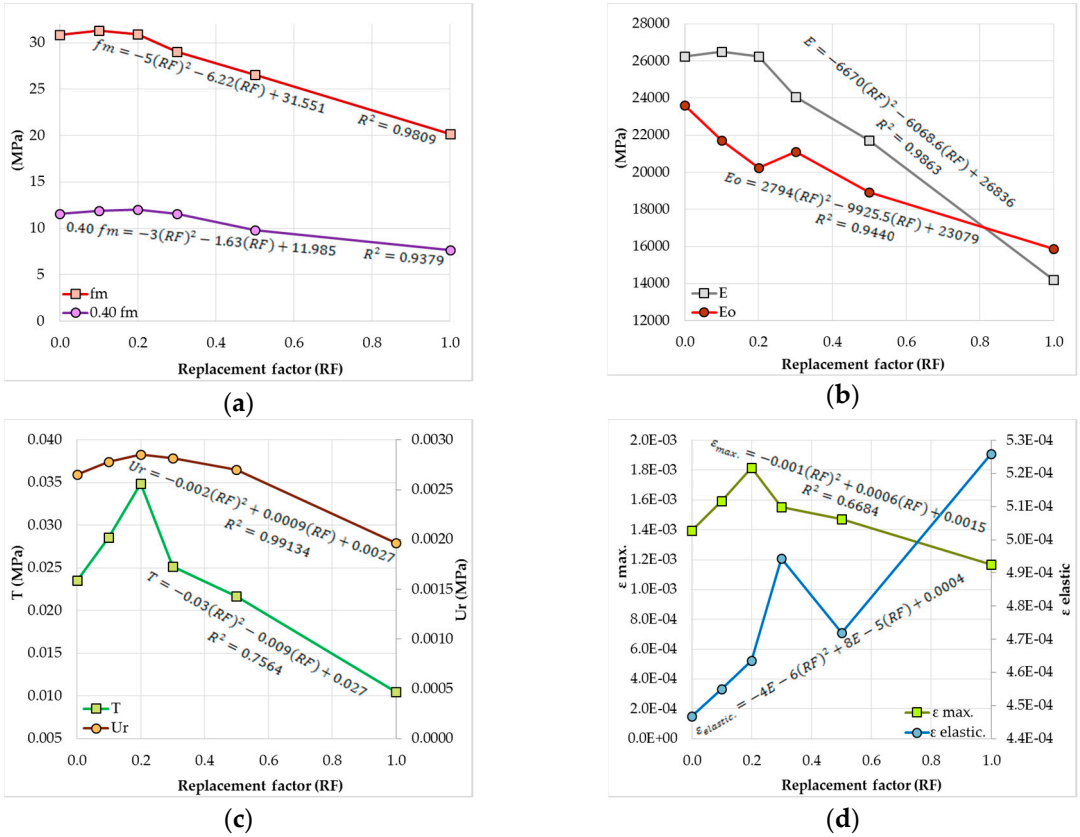

Figure 9. Graphs of the different properties of the RCM vs RF.

3.4. Determining the prediction equations of the RCM

Once the physical, mechanical and σ-ε behavior of the different RCM had been obtained, the focus became the study and establishment of the prediction equations of behavior by means of the prescription, use and determination of the relationship of its properties, as well as the proposal of new coefficients (proper to the RCM). Similarly, numerical equations describing the curve, both in the elastic and plastic range up to the failure load, were determined for all the variables studied.

In order to obtain the prediction equations various pre-existing configurations for the usual concrete were evaluated, intending to optimize their adaptation to mortars and recycled materials; similarly (taking the previously acquired physical and mechanical properties into account) new combinations were also evaluated with the aim of finding those which best described and predicted the σ-ε behavior of the RCM. Finally, apart from establishing the refined prediction equations (PE_r) (for each XX% studied in this research), these were distinguished by means of correction coefficients (C_C); thus aiding their exactitude and precision in predicting the RCM.

To obtain them, it was necessary to use algorithms of numerical approximation by sequencing in cycles with correction criteria known as optimizers, in particular those provided by Solver [50]. This is software which forms part of the command or scenario analysis tools which aid in choosing the best method to make or determine a behavior law. Specifically, using Solver it was possible to find the theoretical constants (T_C) of the conceptual models or predictive equations that represented the behavior of the real values obtained in the experimental campaign. Once the logical conditions (or limitations) of the test had been satisfied and the studio series validations had been carried out, the results obtained from the process were the coefficients that satisfied these pre-established limits. The process included:

Defining the proposed configuration to be resolved (objective equation, O_E). The order, position and variables to be considered were tested according to pre-established logical criteria of the UM behavior, as observed in equation (4).

$$O_E = (T_C) * Study\ \ configuration \quad (4)$$

Where T_C is conditioned to be a whole value.

The PEr to be determined was prescribed with two coefficients or adjustment constants: the first constant (T_C) was limited by the maximum and minimum possible values of the particular evaluation of each group of experimental values obtained (established on the basis of data in **Table 4**), and when possible this coefficient was forced to be a whole number (simplicity in the equation); the second constant, C_C, corresponds to a refining of the OE, allowing it to be sensitive to XX%; see equation (5).

$$PE_r = (T_C) * (C_C) * Study\ \ configuration \quad (5)$$

Stringent conditions for analysis were limited to the following: the values of the variables considered in the O_E were limited by the maximum and minimum of each real experimental result (**Table 4**); the value of O_E with which the adjustment process was initiated was tested with four possible approximation processes: maximum and minimum values, average value of all and the average of the maximum and minimum extremes; all obtained from the real experimental campaign. As an algorithm or method of solving the O_E, of the available algorithms (non-linear method: for adjusting softened non-linear behavior; simple method: for adjusting linear problems; and the evolutive method: for non-linear and disperse behavior), the non-linear method was used as being closest to the behavior of the real experimental values.

Finally, as parameters of the iteration of the applied algorithm the following specifications were defined: the minimum acceptable value of error in the convergence of the O_E equal to or less than 0.0001 (average figure of the last five iterations); evaluation of the iterations i+1: it was established that the new value of the variables to be tested should be determined by means of a forward difference approximation; and finally the initial test values of the variables to be evaluated in the O_E were set as equal for all with a value equal to zero (hypothesis of test values corresponding to the same study phenomenon).

When the O_E with its constant T_C has been obtained, the value of the distinctive constant C_C is determined from the relationship between the real experimental value for each sample with different XX% and the theoretical value of the established O_E; giving as a result as many O_E (with distinctive C_C) as RCM studied, with equation (6).

$$C_C = real\ \ experimental\ \ value\ \ of\ \ the\ \ CRMXX\%/value\ \ obtained\ \ from\ \ the\ \ O_E \quad (6)$$

Where $0 \leq XX\% \leq 100$.

These O_E with distinctive C_C (PE_r) were compared with the real experimental values, the difference being called the Error Differential (E_D) of exactitude obtained from equation (7).

$$E_D = PE_r - \ \ real\ \ value\ \ of\ \ the\ \ experimental\ \ campaign\ \ for\ \ each\ \ CRMXX\% \quad (7)$$

Where $0 \leq XX\% \leq 100$.

Taking into account the group of the E_D established for each PE_r and real test, their standard deviation, S, was determined with equation (8) and the Relationship (R) of the average of E_D ($\overline{X}$) with respect to the average of the real experimental values ($\overline{X}_r$) (in percentage, see equation (9)); it is the criteria (S and R) and the agreement between the experimental and simulated grap, which define, firstly, the criteria for defining the best approximation process for configuring the target equation analyzed and, secondly, those for choosing, from the different configurations, the O_E which is the most appropriate, accurate and similar to the real experimental values.

$$S = \sqrt{\sum_{XX\%=0}^{XX\%=100} (X_{XX\%} - \bar{X})^2/n - 1} \quad (8)$$

Where n is the number of real tests carried out; $\bar{X}$ the average of the E_D and X the E_D for each XX% of the study.

$$R\ \ (\%) = \ \ (\bar{X}/\bar{X}_r) * 100 \quad (9)$$

Where $\bar{X}$ is the average of the E_D and $\bar{X}_r$ the average of the real experimental values.

From the results of the previous procedures for obtaining the PE_r, the following equations were established:

The static modulus of elasticity (equation (10), established by means of the real properties of fm and ρ; and being defined as PE_r through the use of the C_C (see **Table 5**, in column E) for each RCM. The coefficients C_C from XX% ≥ 30 show significant reductions which will establish differences in the PE_r.

$$E = 5521C_C * \sqrt{0.40\ \ fm * \rho} \tag{10}$$

In the specific case of the $\varepsilon_{elastic}$ it was decided to establish two types of PE_r, as the real experimental results did not converge satisfactorily for all the RCM studied; therefore the first of the equations (equation (11) is valid for 0 ≤ XX% ≤ 30, and the equation (12) is applied for 30 ≤ XX% ≤ 100. In both cases, the equations follow similar proposals of variables, and the C_C constants to be used for each RCM may be found in **Table 5**, column $\varepsilon_{elastic}$.

$$\varepsilon_{elastic} = C_C * 0.40\ \ fm/E \tag{11}$$

$$\varepsilon_{elastic} = 0.007C_C * 0.40\ \ fm/\sqrt{E} \tag{12}$$

Regarding the U_r, the proposed equation (13) allows, along with the coefficient C_C of **Table 5** column U_r, the capacity of the different RCM to absorb or transform the energy or workload to be established. In the particular case of C_C = 100%, this is the coefficient that can cause a greater variation in this property.

$$U_r = 5C_C * 0.40\ \ fm/E \tag{13}$$

For property T, equation (14) has been formulated, based on a formulation of the area of a triangle which, along with the coefficients C_C, allows it to be refined for the different RCM.

$$T = 0.62CC * fm * \varepsilon_{max.} \tag{14}$$

Table 5. C_C values for application in PE_r equations of the RCM.

Study variables	Corrector coefficient (C_C for mechanical properties of RCM)			
	E	$\varepsilon_{elastic}$	U_r	T
UM	0.9817	0.9380	1.0086	0.6651
RCM10	0.9915	0.9553	1.0572	0.8075
RCM20	0.9817	0.9734	1.0855	0.9880
RCM30	0.8999	1.0380	1.0716	0.7127
RCM50	0.8126	0.9910	1.0291	0.6129
RCM100	0.5308	1.1043	0.7480	0.2968

The graph in **Figure 10** shows the proposed prediction equation of E for the RCM (equation (10)), as well as the real experimental values of the research campaign. The equation chosen was that which achieved the best convergence, and graphically it is closer to the line of the real experimental values (see the other equations considered). Similarly, the graph shows the results of other previously-mentioned studies; although unfortunately these were proposed with different variables and parameters (shown in the graph), which makes it difficult for the proposed equation to fit (or explain) all of them, although the trend is similar in several [16][22][51]. Further research will be necessary, and new simulations with different parameters of adjustment and refinement should be performed. The established equation, therefore, could be applied to predicting E in the RCM with a c/a close to 1:4, for density values of the RCM in hardened state between 1.95 ≤ ρ ≤1.53 Kg/cm^3 and for replacement values of UA by CA between 0 ≤ XX% ≤ 100.

Preprints (www.preprints.org) | NOT PEER-REVIEWED | Posted: 28 November 2016 doi:10.20944/preprints201611.0143.v1

Peer-reviewed version available at Materials 2016, 9, 1029; doi:10.3390/ma9121029

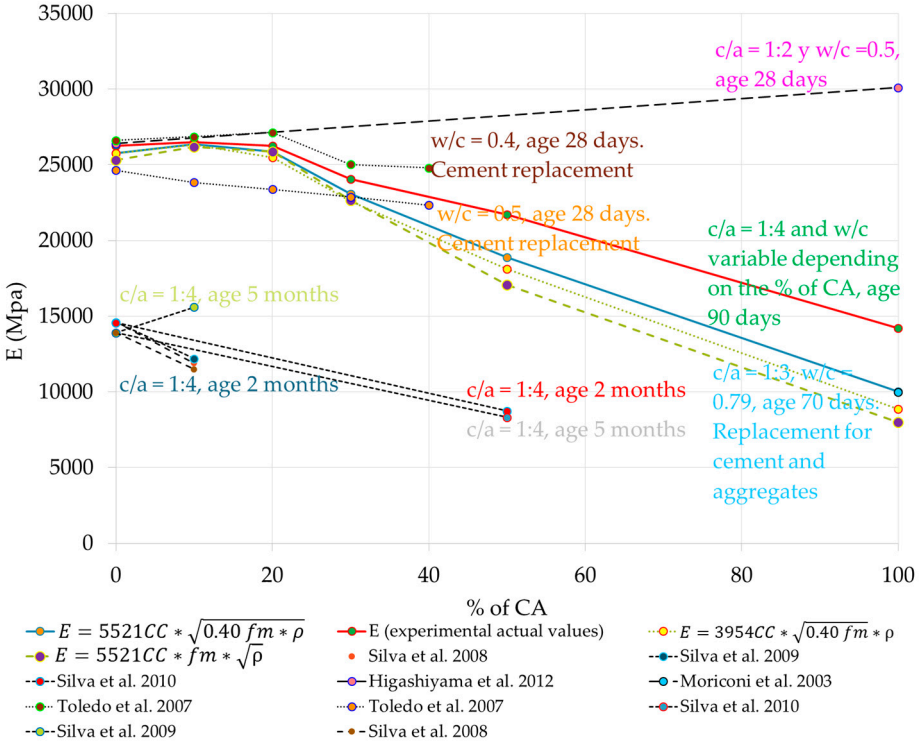

Figure 10. E prediction equation for RCM confronted with real experimental data, and reported in other investigations

Finally, the analytical expression of the curve of the σ-ε relationship of the RCM studied was obtained with the results of **Table 4** (values of E and Eo), using in its conception the proposal by Fanella D. A. & Naaman A. E. [46] for this objective (equation (15).

$$Y = [AX + BX^2/1 + CX + DX^2] \quad (15)$$

In the previous equation the constants of use (A, B, C y D, see equations (16) (17) (18) and (19)) are established, between the proportions of the mechanical properties of the RCM and those of the mathematical and geometrical parameters that produce the curve of an equation fitting the behavior of σ-ε; and X is the value of the deformation in the graph of the real experimental E for the particular point to be determined on the theoretical curve.

$$A_1 = E/E_o \quad (16)$$

$$B_1 = 0.45 - 0.41/A_1 + 0.20/{A_1}^2 \quad (17)$$

$$C_1 = A_1 - 2 \quad (18)$$

$$D_1 = B_1 + 1 \quad (19)$$

Using equation (15) to define the curve of the behavior to be studied and the real experimental values of the RCM, equation (20) (O_E) is defined, which has the constant belonging to the RCM (T_C) family of data (see **Table 6**); its determination was obtained through a similar calculation process with the Solver tool.

$$O_E = (T_C) * [AX + BX^2/1 + CX + DX^2] \quad (20)$$

Where *X* is equal to ε.

To achieve better prediction of the different RCM, a PE_r (equation (21)) has been established by means of the particular constants C_C (**Table 7**) of each XX%, to which the previously indicated process was applied.

Preprints (www.preprints.org) | NOT PEER-REVIEWED | Posted: 28 November 2016 doi:10.20944/preprints201611.0143.v1

Peer-reviewed version available at Materials 2016, 9, 1029; doi:10.3390/ma9121029

$$PE_r = (T_C) * (C_C) * [AX + BX^2/1 + CX + DX^2] \quad (21)$$

Once the processes had been applied, it was necessary to establish three different equations (and Tc) to better adjust the numerical predictions to the real experimental results: two equations are established with respect to the prediction of σ in the σ-ε curve of the RCM until the elastic range ($\sigma_{elastic}$); one for 0 ≤ XX% ≤ 50 and another for XX% = 100. For σ of the curve to maximum of failure (σ_{max}) a single equation is established for all the XX% (of less precision) (see **Table 6** and **Table 7**).

Table 6. Values of the constants for each of the curves.

PE_r of the curve σ-ε	Application	Tc (for the σ-ε curve of the RCM)	A	B	C	D
PE_r for $\sigma_{elastic}$	0 ≤ XX% ≤ 50	16337	0.893	0.242	-0.704	1.253
PE_r for $\sigma_{elastic}$	XX% = 100%	16337	1.245	0.253	-0.704	1.242
PE_r for σ_{max}	0 ≤ XX% ≤ 100	13113	1.179	0.253	-0.704	1.242

Table 7. Values Cc for the different percentages of CA.

	Corrector coefficient (Cc for σ-ε curve of the RCM)	
XX%	**Cc para PE_r hasta $\sigma_{elastic}$**	**Cc para PE_r hasta $\sigma_{max.}$**
0	1.7739	1.0962
10	1.8005	1.1126
20	1.7788	1.0992
30	1.6677	1.0306
50	1.5276	0.9440
100	0.7174	0.7174

The σ-ε curves of the RCM studied by means of the previously-determined simulation equations are shown in **Figure 11**. In both cases, their profiles maintain the order established according to XX% used; likewise establishing a grouping between the curves showing similar behaviour (0 ≤ XX% ≤ 20), afterwards distancing them proportionally in accord with XX% (30 ≤ XX% ≤ 100).

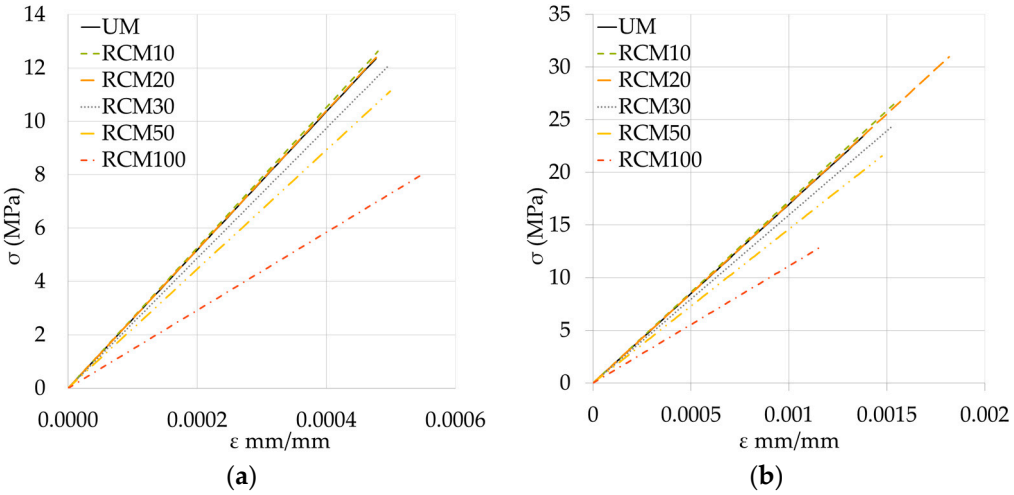

Figure 11. Curve σ-ε simulated for the RCM: (**a**) up to $\sigma_{elastic}$, (**b**) up to $\sigma_{max.}$

5. Conclusions

Based on the experimental data obtained and the numerical processes carried out, the following conclusions can be presented:

The density of the RCM is less than that of the UM, this being inversely correlative to the content of CA; this reduction in density has been attributed to the low density of the CA.

The behavior of the mechanical property of fm responds to three different groupings in terms of CA replacement: with small replacements (10 to 20%) the RCM show similar behavior, even managing to occasionally pass the UM; for intermediate content replacements (30 to 50%) losses in strength of between 6 and 14% may occur; and finally for a total replacement the losses can be significant with respect to the UM (35% less). In the previous behavior, the study of the ITZ in SEM images validates the hypothesis that the strength increases of the RCM can be attributed to the possible pozzolanic reaction of the CA, causing a 'filling' effect in the matrix and reducing its porosity; on the contrary, a less dense ITZ can be seen for high contents, possibly meaning greater porosity in this area which, combined with the low density of the aggregates, leads to a lower fm in RCM with high contents.

The σ-ε behavior of RCM is similar to that shown by a UM, and is the closest to the RCM10 and RCM20: in the case of σ, the RCM10 obtained values even higher than the UM. As for ε, this increases as the percentage of CA is increased, to a maximum of 20%; with CA contents CA ≥ 30%, losses inversely proportional to the content of the CA are obtained. The results of E, obtained from the σ-ε curves, show similar behavior to that shown by the property of fm; for the RCM10 an increase of 1%, for the RCM20 values similar to the UM, and for RCM with CA ≥ 30% the losses are established in the range of 8 to 46%.

The results of the properties of the RCM that were obtained by means of the σ-ε curves have shown increases, while the CA content has been increased until 20%; when the replacement passes 30% the values of each of the properties is inferior regarding the UM. This data has made it possible to formulate predictive equations regarding the percentage of CA, which (quickly and simply) provide values close to the different RCM.

By means of numerical analysis, two constants for use in predictive equations have been obtained, which allow the different properties of the RCM to be related; the first of them is the theoretic constant which represents the behavior of the real values obtained during the experimental campaign of the CA, and the other allows exactitude and precision for each of the RCM with its respective percentage of CA. Specifically, for the predictive equation of E, this cannot be corroborated using the results of previous studies, as these have been proposed with different variables and parameters, although in some cases similar trends are evident.

The analytical expressions obtained from the σ-ε curve of the studied RCM allows prediction of the curves in the elastic range, up to their failure point; thereby easing the study, design and calculation of the constructive elements that these mortars include in their design.

Acknowledgments: The authors thank CONACYT for its doctoral scholarship program, the Polytechnic Higher School of Building Construction of Barcelona-UPC, the Department of Architectonic Constructions II-EPSEB-UPC, the School of Engineering Mochis-UAS and, finally, the program of Young Doctors-UAS.

Author Contributions: F. Guadalupe Cabrera-Covarrubias (B, C, D), J. Manuel Gómez-Soberón (A, B, C, D, F), J. Luis Almaral-Sánchez (B, E, F), S. Paola Arredondo-Rea (B, C.), M. Consolación Gómez-Soberón (B, C), Ramón Corral-Higuera (B, E). Type of contribution: A - Research concept and design. B - Collection and/or assembly of data. C - Data analysis and interpretation. D - Writing the article. E - Critical revision of the article. F - Final approval of article.

Conflicts of Interest: The authors declare no conflict of interest.

Abbreviations

The following abbreviations are used in this manuscript:

σ-ε: Stress-strain
CA: Recycled aggregates of ceramic
UA: Usual aggregates

RCM: Recycled ceramic mortars
CePo: Ceramic powder
c/a: Cement/aggregate
w/c: Water/cement
fm: Compressive strength
PS: Particle size
E: Module of elasticity or Young
$\varepsilon_{elastic}$: Elastic deformation
0.40 fm: 40% of the maximum load of failure
$\varepsilon_{max.}$: Maximum deformation of failure
U_r: Resiliency
T: Toughness
M_{OD}: Bulk density in oven-dry condition
M_{SSD}: Bulk density in saturated-surface-dry condition
D_{OD}: Density in oven-dry condition
D_{SSD}: Density in saturated-surface-dry condition
UM: Usual mortar
SEM: scanning electron microscope
G: Grout
ITZ: Interfacial transition zone
XRD: X-ray diffraction
RF: Replacement factor
PE_r: Refined prediction equations
C_C: Correctors coefficients
T_C: Theoretical constants
O_E: Objective equation
$\sigma_{elastic}$: Stress in the elastic range
$\sigma_{max.}$: Up to maximum stress of failure

References

[1] Higashiyama, H.; Yamauchi, K.; Sappakittipakorn, M.; Sano, M.; Takahashi, O. A visual investigation on chloride ingress into ceramic waste aggregate mortars having different water to cement ratios. *Constr. Build. Mater.* **2013**, *40*, 1021–1028, DOI: 10.1016/j.conbuildmat.2012.11.078.

[2] Ay N.; Ünal, M. The use of waste ceramic tile in cement production. *Cem. Concr. Res.* **2000**, *30*, 497–499, DOI: 10.1016/S0008-8846(00)00202-7.

[3] Lavat, A.E.; Trezza, M.A.; Poggi, M. Characterization of ceramic roof tile wastes as pozzolanic admixture. *Waste Manag.* **2009**, *29*, 1666–74, DOI: 10.1016/j.wasman.2008.10.019.

[4] Lázaro, C.; Trilles, V.R.; Gómez F. Incorporación de residuos derivados de la fabricación cerámica y del vidrio reciclado en el proceso cerámico integral. *Boletín la Soc. Española Cerámica y Vidr.* **2012**, *51*, 139–144, DOI: 10.3989/cyv.202012.

[5] Silva, J.; Brito, J.; Veiga, R. Recycled Red-Clay Ceramic Construction and Demolition. *J. Mater. Civ. Eng.* **2010**, *22*, 236–244, DOI: 10.1061/(ASCE)0899-1561(2010)22:3(236).

[6] Corinaldesi, V. Environmentally-friendly bedding mortars for repair of historical buildings. *Constr. Build. Mater.* **2012**, *35*, 778–784, DOI: 10.1016/j.conbuildmat.2012.04.131.

[7] Wild, S.; Khatib, J.M.; O'Farrell, M. Sulphate resistance of mortar, containing ground brick clay calcined at different temperatures. *Cem. Concr. Res.* **1997**, *27*, 697–709, DOI: 10.1016/S0008-8846(97)00059-8.

[8] O'Farrell, M.; Wild, S.; Sabir, B.B. Resistance to chemical attack of ground brick-PC mortar Part I . Sodium sulphate solution. *Cem. Concr. Res.* **1999**, *29*, 1781–1790, DOI: 10.1016/S0008-8846(99)00170-2.

[9] O'Farrell, M.; Wild, S.; Sabir, B.B. Resistance to chemical attack of ground brick ± PC mortar Part II .

Synthetic seawater. *Cem. Concr. Res.* **2000**, *30*, 757–765, DOI: 10.1016/S0008-8846(00)00245-3.

[10] O'Farrell, M.; Wild, S.; Sabir, B.B. Pore size distribution and compressive strength of waste clay brick mortar. *Cem. Concr. Compos.* **2001**, *23*, 81–91, DOI: 10.1016/S0958-9465(00)00070-6.

[11] Moriconi, G.; Corinaldesi, V.; Antonucci, R. Environmentally-friendly mortars: a way to improve bond between mortar and brick. *Mater. Struct.* **2003**, *36*, 702–708, DOI: 10.1007/BF02479505.

[12] Turanli, L.; Bektas, F.; Monteiro P.J.M. Use of ground clay brick as a pozzolanic material to reduce the alkali–silica reaction. *Cem. Concr. Res.* **2003**, *33*, 1539–1542, DOI: 10.1016/S0008-8846(03)00101-7.

[13] O'Farrell, M.; Sabir, B.B.; Wild, S. Strength and chemical resistance of mortars containing brick manufacturing clays subjected to different treatments. *Cem. Concr. Compos.*, **2006**, *28*, 790–799, DOI: 10.1016/j.cemconcomp.2006.05.014.

[14] Toledo Filho, R.D.; Gonçalves, J.P., Americano, B.B.; Fairbairn, E.M.R. Potential for use of crushed waste calcined-clay brick as a supplementary cementitious material in Brazil. *Cem. Concr. Res.* **2007**, *37*, 1357–1365, DOI: 10.1016/j.cemconres.2007.06.005.

[15] Puertas, F.; García-Díaz, I.; Palacios, M.; Martínez-Ramírez, S. Empleo de residuos cerámicos como materia prima alternativa para la fabricación de clínker de cemento portland. *Cem. Hormigón* **2007** , *907*, 20–34, Available online: https://dialnet.unirioja.es/servlet/articulo?codigo=2474572 (accessed on 2 march 2016).

[16] Silva, J.; Brito, J.; Veiga, R. Fine ceramics replacing cement in mortars Partial replacement of cement with fine ceramics in rendering mortars. *Mater. Struct.* **2008**, *41*, 1333–1344, DOI: 10.1617/s11527-007-9332-z.

[17] Pereira-de-Oliveira, L.A.; Castro-Gomes, J.P.; Santos, P.M.S. The potential pozzolanic activity of glass and red-clay ceramic waste as cement mortars components. *Constr. Build. Mater.* **2012**, *31*, 197–203, DOI: 10.1016/j.conbuildmat.2011.12.110.

[18] Wang G.; Tian, B. Effect of Waste Ceramic Polishing Powder on the Properties of Cement Mortars. Proceedings of the International Conference on Energy and Environment Technology ICEET '09, 2009, Guilin, Guangxi, 2009, Publisher: IEEE, 101–104, DOI: 10.1109/ICEET.2009.31.

[19] Kumavat H.R.; Sonawane,Y.N. Feasibility Study of Partial Replacement of Cement and Sand in Mortar by Brick Waste Material. *Int. J. Innov. Technol. Explor. Eng.* **2013**, *2*, 17–20, Available online: https://www.oalib.com/paper/2173846#.V5ncxfmLSUk (accessed on 2 march 2016).

[20] Jiménez, J.R.; Ayuso, J.; López, M.; Fernández, J.M.; Brito, J. Use of fine recycled aggregates from ceramic waste in masonry mortar manufacturing. *Constr. Build. Mater.* **2013**, *40*, 679–690, DOI: 10.1016/j.conbuildmat.2012.11.036.

[21] Bektas, F.; Wang, K.; Ceylan, H. Effects of crushed clay brick aggregate on mortar durability. *Constr. Build. Mater.* **2009**, *23*, 1909–1914, DOI: 10.1016/j.conbuildmat.2008.09.006.

[22] Silva, J.; Brito, J.; Veiga, R. Incorporation of fine ceramics in mortars. *Constr. Build. Mater.* **2009**, *23*, 556–564, DOI: 10.1016/j.conbuildmat.2007.10.014.

[23] Corinaldesi, V. Mechanical behavior of masonry assemblages manufactured with recycled-aggregate mortars. *Cem. Concr. Compos.* **2009**, *31*, 505–510, DOI: 10.1016/j.cemconcomp.2009.05.003.

[24] Higashiyama, H.; Yagishita, F.; Sano, M.; Takahashi, O. Compressive strength and resistance to chloride penetration of mortars using ceramic waste as fine aggregate. *Constr. Build. Mater.* **2012**, *26*, 96–101, DOI: 10.1016/j.conbuildmat.2011.05.008.

[25] Gesoğlu, M.; Güneyisi, E.; Özturan, T. Effects of end conditions on compressive strength and static elastic modulus of very high strength concrete. *Cem. Concr. Res.* **2002**, *32*, 1545–1550, DOI: 10.1016/S0008-8846(02)00826-8.

[26] Demir F.; Armagan Korkmaz, K. Prediction of lower and upper bounds of elastic modulus of high

strength concrete. *Constr. Build. Mater.* **2008**, 22, 1385–1393, DOI: 10.1016/j.conbuildmat.2007.04.012.

[27] Suto, H. Relation between Modulus of Elasticity and Compressive Strength of Ultrahigh-Strength Mortar with Mixed Silicon Carbide as Fine Aggregate. *J. Mater. Sci. Technol.* **2001**, *17*, 579–580, Available online: https://www.jstage.jst.go.jp/article/jinstmet1952/63/8/63_8_1083/_article (accessed on 2 march 2016).

[28] Corinaldesi, V.; Giuggiolini, M.; Moriconi, G. Use of rubble from building demolition demolition in mortars. *Waste Manag.* **2002**, *22*, 893–899, DOI: 10.1016/S0956-053X(02)00087-9.

[29] Zhou J.; Chen, X. Stress-Strain Behavior and Statistical Continuous Damage Model of Cement Mortar under High Strain Rates. *J. Mater. Civ. Eng.* **2013**, *1*, 120–130, DOI: 10.1061/(ASCE)MT.1943-5533.0000570.

[30] Martínez P.; Azuaga, M. Medición del módulo de elasticidad de Young. Available online: http://www.fisicarecreativa.com/informes/infor_mecanica/young97.pdf. (accessed on 10 january 2016).

[31] Candelario, M.P. Propiedades mecánicas de los materiales," *METALOGRAFÍA – UNIVERSIDAD TECNOLÓGICA DE PEREIRA*, 2012. Available online: http://blog.utp.edu.co/metalografia/2-propiedades-mecanicas-de-los-materiales/. (accessed on 04 April 2015).

[32] Lima, P.R.L.; Toledo, R.D.; Melo, J.A. Compressive Stress-strain Behaviour of Cement Mortar-composites Reinforced with Short Sisal Fibre. *Mater. Res.* **2014**, *17*, 38–46, DOI: 10.1590/S1516-14392013005000181.

[33] Serrano-guzmán M.F.; Perez-Ruiz, D.D. Análisis de sensibilidad para estimar el módulo de elasticidad estático del concreto. *Concreto y Cem. Investig. y Desarro.* **2010**, *2*, 17–30, Available online: http://www.imcyc.com/ccid.ojs/index.php/ccid/article/view/13. (accessed on 30 April 2015).

[34] *Standard Specification for Aggregate for Masonry Mortar;* ASTM C144-99; American Society for Testing and Materials: West Conshohocken, PA, 1999.

[35] *Standard Test Method for Density, Relative Density (Specific Gravity), and Absorption;* ASTM C128-04a; American Society for Testing and Materials: West Conshohocken, PA, 2004.

[36] *Standard Test Method for Sieve Analysis of Fine and Coarse Aggregates;* ASTM C136-06. American Society for Testing and Materials: West Conshohocken, PA, 2006.

[37] *Standard Test Method for Materials Finer than 75-µm (No. 200) Sieve in Mineral*; ASTM C117-95. American Society for Testing and Materials: West Conshohocken, PA, 1995.

[38] *Parte 1: Composición, especificaciones y criterios de conformidad de los cementos comunes;* AENOR, UNE-EN 197-1; Asociación Española de Normalización y Certificación: Madrid, España, 2011.

[39] Sagoe-Crentsil, K.K.; Brown, T.; Taylor, A.H. Performance of concrete made with commercially produced coarse recycled concrete aggregate. *Cem. Concr. Res.* **2001**, *31*, 707–712, DOI: 10.1016/S0008-8846(00)00476-2.

[40] García-González, J.; Rodríguez-Robles, D.; Juan-Valdés, A.; Morán del Pozo, J.M.; Guerra-Romero, M.I. Pre-saturation technique of the recycled aggregates: Solution to the water absorption drawback in the recycled concrete manufacture. *Materials* **2014**, *7*, 6224–6236, DOI: 10.3390/ma7096224.

[41] *Standard Specification for Flow Table for Use in Tests of Hydraulic Cement*; ASTM C230/C230M-03; American Society for Testing and Materials: West Conshohocken, PA, 2003.

[42] *Standard Test Method for Air Content of Freshly Mixed Concrete by the Pressure Method*; ASTM C231-08b; American Society for Testing and Materials: West Conshohocken, PA, 2008.

[43] *Parte 10: Determinación de la densidad aparente en seco del mortero endurecido;* AENOR, UNE-EN 1015-10; Asociación Española de Normalización y Certificación: Madrid, España, 2000.

[44] *Determinación de la densidad real y aparente y de la porosidad abierta y total*; AENOR, UNE-EN 1936; Asociación Española de Normalización y Certificación: Madrid, España, 2007.

[45] *Standard Test Method for Compressive Strength of Hydraulic-Cement Mortars (Using Portions of Prisms Broken in Flexure)*; ASTM C349-97. American Society for Testing and Materials: West Conshohocken, PA, 1997.

[46] Fanella D.A.; Naaman, A.E. Stress-strain Properties of Fiber Reinforced Mortar in Compression. *ACI J.*, **1985**, *82*, 475–483, Available online: https://www.concrete.org/publications/internationalconcreteabstractsportal.aspx?m=details&ID=10359. (accessed on 8 April 2015).

[47] Ávila, O.; Carrillo, J.; Alcocer, S.M. Rehabilitación de muros de concreto usando CRFA: ensayos en mesa vibradora. *Concreto y Cem. Investig. y Desarro.* **2011**, *2*, 2–17, Available online: http://www.redalyc.org/articulo.oa?id=361233548001. (accessed on 5 April 2015).

[48] Corinaldesi V.; Moriconi, G. Behaviour of cementitious mortars containing different kinds of recycled aggregate. *Constr. Build. Mater.* **2009**, *23*, 289–294, DOI: 10.1016/j.conbuildmat.2007.12.006.

[49] *Norme Française Homologué, "Mesure du module d"élasticité dynamique"*; AFNOR, NF B10-511; Association française de Normalisation: Francia, 1975.

[50] I. Frontline Systems, "Solver," *FrontlineSolvers*, 2016. Available online: http://www.solver.com. (accessed on 1 july 2015).

[51] Silva, J.; Brito, J.; Veiga, R. Recycled Red-Clay Ceramic Construction and Demolition Waste for Mortars Production. *J. Mater. Civ. Eng.* **2010**, 22, 236–244, DOI: 10.1061/(ASCE)0899-1561(2010)22:3(236).